Twilight and daytime colors of the clear sky

Raymond L. Lee, Jr.

Digital image analysis of the cloudless sky's daytime and twilight chromaticities challenges some existing ideas about sky colors. First, although the observed colors of the clear daytime sky do lie near the blackbody locus, their meridional chromaticity curves may resemble it very little. Second, analyses of twilight colors show that their meridional chromaticity curves vary greatly, with some surprising consequences for their colorimetric gamuts.

Key words: Atmospheric optics, clear-sky chromaticities, blue sky, twilight colors, digital image analysis.

Introduction

Several years ago Bohren and Fraser[1] asked "How can anyone have the audacity to write about colors of the sky in the year 1985?" Nearly a decade later, writing about sky colors is no less audacious—and no less necessary. For all the myths and canards that Bohren and Fraser helped dispel about sky color, new (or even reinvented) ones can readily take their place, especially in the absence of suitable quantitative observations.

In the past, researchers have variously measured spectral irradiances of the sky itself, of direct sunlight, or of their combination.[2–8] The latter spectra are usually, if not consistently, labeled daylight as distinct from skylight or direct sunlight.[9] Our interests here diverge from the earlier work on two counts: (1) we are concerned exclusively with the chromaticities of skylight, rather than daylight, and (2) we derive those chromaticities from spectral radiances, rather than irradiances. In this study, we have not directly measured how skylight's partial linear polarization affects its color and luminance distribution.

In fairness, our research is a luxury made possible by equipment unavailable in the past. Techniques of photographic image analysis[10] and the availability of fast-scanning, narrow field-of-view (FOV) spectroradiometers[11] let us make spatially and spectrally detailed measurements of sky radiances. In particular, we are interested in clear-sky chromaticity curves generated by scanning along sky meridians (i.e., across zenith angles at a fixed azimuth). For convenience, we call this type of chromaticity curve a *meridional chromaticity scan.* Because our scans are confined to within 20° of the horizon, we use elevation angle rather than zenith angle in our analyses.

Some of our meridional scans were made near midday, whereas others were made near sunset. Both sets of measurements present us with some unexpected results. Although our findings largely support Bohren and Fraser's assertions, they bring into question some earlier claims about twilight colors.[12,13] We also examine a subtle (and, I suspect, unintended) implication of earlier displays of daylight chromaticities[2–6,8]

Measuring Clear-Sky Chromaticities

Our examination of sky colors begins by restating a definition introduced earlier.[14] We define the normalized colorimetric gamut $\hat{g}$, which attempts to quantify the range of colors that we encounter in a scene. First we calculate a chromaticity curve's unnormalized colorimetric gamut g by finding the curve's average chromaticity [here, its mean CIE (Commission Internationale de l'Eclairage) 1976 u', v']. Next we calculate the root-mean-square (rms) Cartesian distance of the curve's chromaticities from its $\overline{u'}$, $\overline{v'}$. Thus for a chromaticity curve of $\mathcal{N}$ points,

$$g = \left\{ \left[\sum_{i=1}^{\mathcal{N}} (u_i' - \overline{u'})^2 + (v_i' - \overline{v'})^2 \right] \Big/ \mathcal{N} \right\}^{1/2}. \quad (1)$$

Like any other chromaticity curve, the spectrum locus also has a colorimetric gamut, g_s. Taking the spectrum locus as an upper limit on color gamut, we use its gamut to normalize any other chromaticity

The author is with the Department of Oceanography, United States Naval Academy, Annapolis, Maryland 21402.

Received 17 September 1993; revised manuscript received 18 November 1993.

0003-6935/94/214629-10$06.00/0.

Report Documentation Page

Form Approved
OMB No. 0704-0188

1. REPORT DATE	2. REPORT TYPE	3. DATES COVERED
18 NOV 1993		**00-00-1993 to 00-00-1993**

4. TITLE AND SUBTITLE	5a. CONTRACT NUMBER
Twilight and daytime colors of the clear sky	5b. GRANT NUMBER
	5c. PROGRAM ELEMENT NUMBER
6. AUTHOR(S)	5d. PROJECT NUMBER
	5e. TASK NUMBER
	5f. WORK UNIT NUMBER
7. PERFORMING ORGANIZATION NAME(S) AND ADDRESS(ES) **United States Naval Academy (USNA),Oceanography Department,Annapolis,MD,21402**	8. PERFORMING ORGANIZATION REPORT NUMBER
9. SPONSORING/MONITORING AGENCY NAME(S) AND ADDRESS(ES)	10. SPONSOR/MONITOR'S ACRONYM(S)
	11. SPONSOR/MONITOR'S REPORT NUMBER(S)

12. DISTRIBUTION/AVAILABILITY STATEMENT
Approved for public release; distribution unlimited

13. SUPPLEMENTARY NOTES

14. ABSTRACT

15. SUBJECT TERMS

16. SECURITY CLASSIFICATION OF:			17. LIMITATION OF ABSTRACT	18. NUMBER OF PAGES	19a. NAME OF RESPONSIBLE PERSON
a. REPORT	b. ABSTRACT	c. THIS PAGE			
unclassified	**unclassified**	**unclassified**	**Same as Report (SAR)**	**10**	

curve's gamut g such that

$$\hat{g} = g/g_s. \tag{2}$$

Thus $\hat{g}$ ranges from 0 to 1, independent of the colorimetric system used ($\hat{g} \equiv 1$ for the spectrum locus). However, the greater a color space's perceptual anisotropy, the less $\hat{g}$ will correspond to our subjective impression of color gamut.

To measure the chromaticities of clear skies, we apply our digital image techniques to color slides such as Plates 41–43. The colorimetric data extracted can be comparable in quality with that derived from spectroradiometers.[10] We make such a comparison in Fig. 1, where two meridional scans of the sky are shown on a CIE 1976 uniform-chromaticity-scale (UCS) diagram.

Figure 1 illustrates both the assets and the liabilities of the photographic technique. The radiometer and photographic chromaticities are taken from a 0.5°-FOV meridional swath of the clear-sky scene shown in Ref. 15, Plate 37. Because the two instruments gathered data from the same source at nearly the same time (University Park, Pa., at ~1605 GMT on 6 October 1992), the resulting chromaticity curves should be almost identical. Obviously they are not. Taking the spectroradiometer data as our reference standard, we find that the photographic chromaticities are slightly purer and their gamut is slightly larger. Specifically, $\hat{g}$ increases from 0.0386 to 0.0519 and mean colorimetric purity increases from 12.6% to to 13.9% (purities are measured with respect of extraterrestrial sunlight with $u' = 0.202, v' = 0.467$).[16]

We cannot ignore the photographic technique's errors in calculating absolute chromaticities. However, much of this error arises from uncertainties in choosing the spectrum of direct and diffuse sunlight radiances L_λ that contributes to skylight. Experience with our algorithm tells us that if we choose a different spectral shape for L_λ (or if we know L_λ accurately), we can move the radiometer and photographic curves in Fig. 1 arbitrarily close together. Even without making such a fortuitous choice, we note that the gamuts and general shapes of the photographic and radiometer chromaticity curves are quite similar.

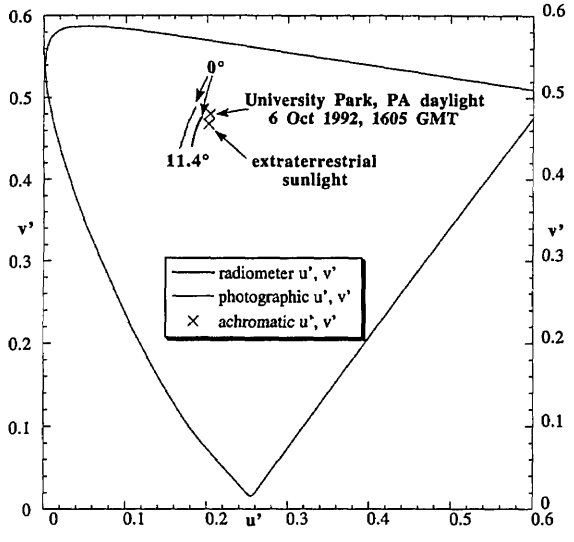

Fig. 1. Comparison of CIE 1976 UCS chromaticity curves derived from photographic and spectroradiometer data for the same 0.5°-FOV meridional clear-sky scan made at ~1605 GMT on 6 October 1992 at University Park, Pa. See Ref. 15, Plate 37 for the original photograph.

If we are primarily interested in comparing the colorimetric shapes and gamuts of sky features, rather than their absolute chromaticities, the photographic technique has clear advantages. Among these are ease and speed of use. Even our fast-scanning radiometer (a visible spectrum often can be acquired in ~0.1 s) requires considerable time to set up, and the 24 chromaticities plotted in Fig. 1 took ~20 min to acquire. Even if we speed up our data acquisition with the radiometer, a color slide (1) requires negligible setup time (Plates 42 and 43 were taken during commercial airline flights), (2) maps an entire scene's radiances in a fraction of a second, and (3) captures ephemeral, low-light phenomena that are invisible to the radiometer.

Observed Colors of Clear Daytime Skies

With the above caveats in mind, we begin our survey of clear-sky chromaticities that are derived from color slides. In Fig. 1 we have marked the view elevation angles of the original slide's topographic horizon (0°) and of its upper edge (11.4°). This range of elevation angles depends on both the horizon's location within the image and on the 35-mm camera's orientation (Plates 37–43 were taken with 50-mm focal-length lenses; see Ref. 15 for Plates 37–40). We use elevation angle measured with respect to the topographic (rather than astronomical) horizon throughout this paper; the two differ at most by a few degrees in Plates 37–43.

Note that we have labeled two achromatic points in Fig. 1. One corresponds to the color of sunlight outside the atmosphere. The second is an estimate of daylight color (direct sunlight plus hemispherically integrated surface light and skylight) at 0° relative azimuth[17] for Fig. 1's time and location. This second achromatic point plausibly describes the average L_λ that contribute to skylight in a multiple-scattering atmosphere. However, because the true L_λ vary with elevation and relative azimuth angles, using a fixed daylight spectrum is not a perfect alternative.

Figure 1's two achromatic points also illustrate why we have used colorimetric gamut $\hat{g}$ rather than, say, mean purity to describe the range of skylight colors. Because both of our achromatic points (and many more besides) are plausible reference chromaticities for calculating skylight purities, we can arrive at almost any mean purity figure that we like in Fig. 1. By contrast, $\hat{g}$ does not require us to invoke an arbitrary white stimulus.

What does Fig. 1 tell us about the behavior of skylight color? First, as is true of most colors in

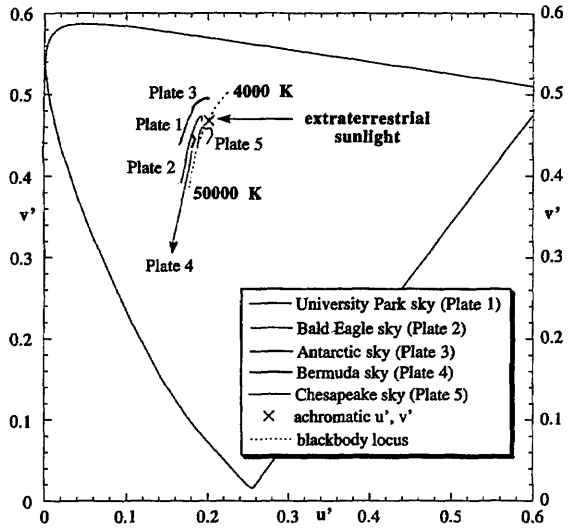

Fig. 2. Chromaticity curves of daytime clear skies for Plates 37–40 (Ref. 15) and Plate 41 are compared with a portion of the blackbody locus. See Fig. 3 for a detailed view of these curves. The color of sunlight outside the atmosphere is marked by an ×.

nature, skylight's gamut and purity are rather small compared to our expectations of them.[18,19] However, note that we have measured chromaticities within only ~11° of the horizon. If we were to extend our analysis to the zenith, the skylight gamut would increase slightly, but not greatly. In fact, the theoretical upper bound on clear-sky purity is ~42% (in the absence of spectrally selective absorption).[1] If we use the chromaticity of extraterrestrial sunlight as our achromatic point, purities from Fig. 1's radiometer data range between 3.0% at 1° elevation and 22.8% at 15° elevation.

Now we have come to our second surprise. Rather than the clear sky having its lowest purity *at* the horizon, here it occurs 1° *above* the horizon. Our canonical molecular atmosphere does not behave this way; there purity decreases monotonically from zenith to horizon (see Ref. 1, Fig. 5). Admittedly, the local minimum of purity at 1° elevation is unlikely to be perceptible because purity increases less than 1% between 1° and the horizon. To see if this chromaticity pattern is a fluke, we now examine several other daytime clear skies.

Figure 2 shows the photographically derived chromaticity curves for Plate 41 and for Plates 37–40 in Ref. 15. Table 1 lists the locales and relevant viewing parameters for these five scenes as well as for two twilight scenes (Plates 42 and 43). Chromaticities have been averaged across a broad range of azimuth angles in each plate (except for Plate 37, in which a simulated 0.5° FOV is used), and the relative azimuths given in Table 1 are for the center of each meridional scan. To convey a sense of the reliability of Fig. 2's chromaticities, Table 1 also lists the standard deviations $\sigma_{u'}$ and $\sigma_{v'}$ of u' and v' about their azimuthal means. Because $\sigma_{u'}$ and $\sigma_{v'}$ are different at each view elevation angle, Table 1 simply reports their average values above the horizon in each scene.

In Fig. 3 we zoom in on Fig. 2's chromaticity curves. Now curves are labeled with the horizon elevation (0°) and the maximum view elevation angle in each scene. The effects of azimuthal averaging are evident in the 0.5°-FOV University Park scan, which is noticeably more erratic than the broader scans. In fact, the University Park chromaticities have been further smoothed by a 10-point moving average to improve their legibility. For all its irregularity, however, the University Park scan is the least surprising of the five daytime chromaticity curves. In each of the others, we are unlikely to recognize the seemingly simple skylight gradients of Plates 38–41. The University Park sky's geographic companion is the sky above Bald Eagle Mountain (see Ref. 15, Plate

Table 1. Summary of Viewing Geometry and Chromaticity Information for Plates 37–43[a]

Plate	Location and Date	Solar Elevation Angle (deg)	Relative Azimuth Angle (deg)	Azimuth Width (deg)	Gamut $\hat{g}$	Mean $\sigma_{u'}$	Mean $\sigma_{v'}$
40, Ref. 15	Hamilton, Bermuda, 2 June 1988	75	50	30.6	0.013	0.00193	0.00497
39, Ref. 15	Antarctic interior (date unknown)	13	100	34.1	0.0219	0.00112	0.00107
41	North Beach, Md., 24 March 1992	4	170	22.4	0.0281	0.00126	0.00305
37, Ref. 15	University Park, Pa., 6 October 1992	42	118	0.5	0.0516	0.00119	0.00418
38, Ref. 15	Bald Eagle Mountain (from University Park, Pa.), 5 February 1987	27	106	32.8	0.083	0.00202	0.00416
43	N of Philadelphia, Pa., 27 December 1991	−2 (e)	5 (e)	22.4	0.131	0.0153	0.0101
42	SW of Manchester, N.H., 19 October 1990	−1 (e)	25 (e)	12.8	0.172	0.00415	0.00842

[a]The solar elevation and relative azimuth angles for each location are determined from solar ephemeris calculations or from photogrammetry. An (e) denotes an estimated angle. Azimuth width is the range of azimuth angles over which azimuthal averaging occurs. Colorimetric gamut $\hat{g}$ and the average standard deviations of u' and v' about their azimuthal means are also listed. Table rows are arranged in order of increasing $\hat{g}$.

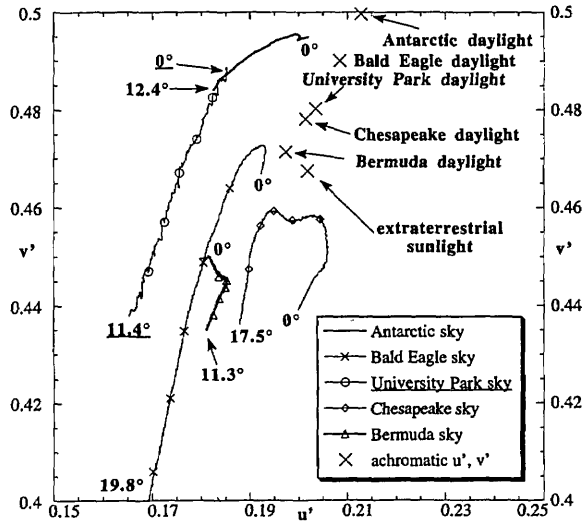

Fig. 3. Detailed view of Fig. 2. The daylight chromaticities (marked with ×'s) are estimated from hemispheric spectral irradiances measured at 0° relative azimuth and at the solar elevations listed in Table 1.

38). However, because of its broader azimuthal average (each chromaticity is averaged over 760 pixels), the Bald Eagle scan is much smoother. This colorimetric smoothness makes the hook shape 0.7° above the Bald Eagle horizon all the more believable intellectually, if not visually.

In fact, relatively sharp bends occur in all of Fig. 3's remaining skylight curves. The hook shape at 2.2° elevation is fairly small in the Antarctic curve (Ref. 15, Plate 39). However, a chromaticity bend at 4.6° elevation dominates the Bermuda curve (Ref. 15, Plate 40). The same is true of the Chesapeake curve (Plate 41), in which a broad bend essentially defines the entire curve and stretches from 9°–2.5° elevation.

Are these chromaticity hooks and bends associated with any other clear-sky features? Before addressing this question, we turn to another, more basic one. Is there any reason to be surprised by the skylight chromaticity curves plotted in Figs. 2 and 3?

Skylight Color, Daylight Color, and a False Conundrum

For readers used to seeing daylight chromaticity scattergrams such as those in Refs. 2–6 and 8, our chromaticity diagrams may be perplexing. In the past, researchers usually have been concerned about where their daylight chromaticities fell with respect to the blackbody locus. This concern suggests, however unintentionally, that the blackbody locus is a template for *any* distribution of daytime clear-sky chromaticities. Yet, as Figs. 2 and 3 make clear, the blackbody locus scarcely begins to describe the tremendous variety of skylight meridional chromaticity curves.

Daylight and skylight chromaticity curves will differ for two basic reasons. First, as noted above, we measure skylight chromaticities over much smaller solid angles than daylight colors. Thus the different patterns evident in skylight and daylight colors are partly due to different viewing directions and FOV's. For example, notice how the daylight chromaticities in Fig. 3, in contrast to the skylight chromaticities, cluster along a line slightly greenward of extraterrestrial sunlight (which is a good spectral proxy for blackbody radiation).

Second, a tendency to connect the dots often drives our reading of scattergrams, especially when correlation coefficients are high, as is true for daylight chromaticity diagrams. In other words, we may easily persuade ourselves that closely spaced chromaticities form a chromaticity curve generated by scanning across the sky. However, a well-defined curvilinear *scatter* of daylight chromaticities implies nothing about the meridional *patterns* of skylight (or even daylight) colors.

Visualizing Luminance in Meridional Skylight Chromaticity Scans

Sharp bends and hooks in skylight chromaticity curves can be easily explained if we examine the chromaticity diagram's implicit third dimension: luminance.[20] Our colorimetric analysis algorithm calculates a spectrally integrated relative luminance, i.e., luminance scaled by that from a reference material. As our scaling luminance, we use the luminance reflected by a Lambertian surface whose reflectance is 100% at all wavelengths. Our algorithm assumes that the same daylight spectrum that generates the observed skylight also illuminates the Lambertian surface (this daylight spectrum will change as the times and places of our photographs change).[10] Clearly skylight is not the result of reflection *per se*, but as a scaling definition, our use of object-color terminology is perfectly acceptable. In Fig. 4, we show how azimuthally averaged relative luminance varies with elevation angle for our five daytime skies.

What are the consequences of combining luminance and chromaticity in one diagram? As Figs. 5–8 indicate, we can immediately see the relationship

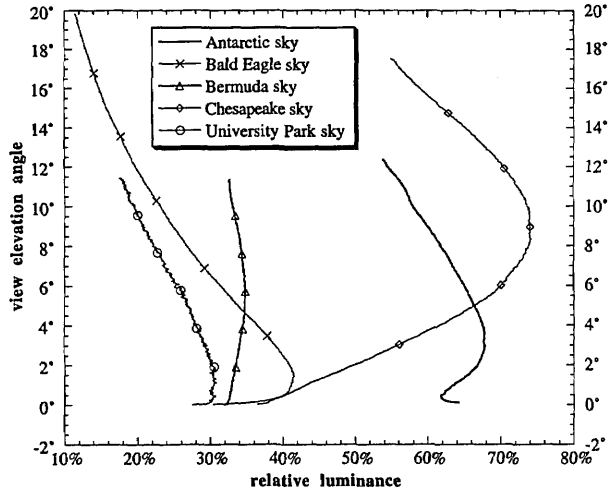

Fig. 4. Relative luminance versus view elevation angle for Plates 37–40 (Ref. 15) and Plate 41. Compare these relative luminances with their stereo representations in Figs. 5–8.

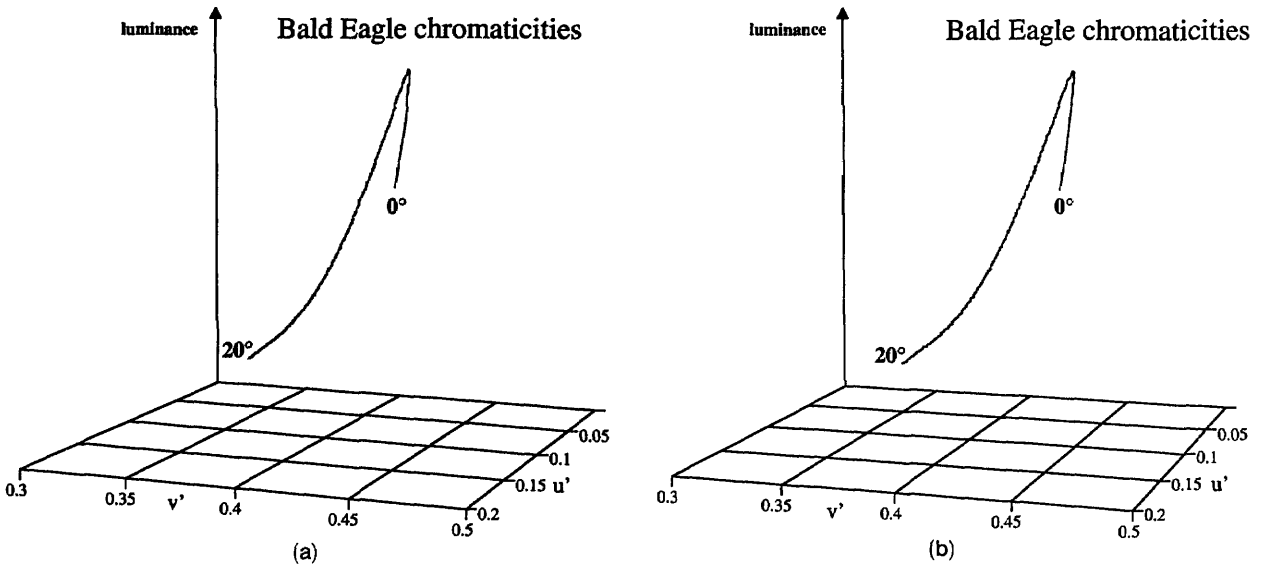

Fig. 5. Stereogram pair of the Bald Eagle Mountain sky's meridional luminance and chromaticity scan (see Ref. 15, Plate 38 for the original photograph). In this figure and in Figs. 6–8 and 12, (a) shows the left-hand side of the stereogram pair and (b) shows the right-hand side of the stereogram pair.

between chromaticity changes and luminance changes, which is a much more realistic way of interpreting sky colors than simply relying on chromaticity alone. In essence, Figs. 5–8 have combined the chromaticity and luminance information of Figs. 3 and 4 into unified plots of this three-dimensional data. Figures 5–8 are presented as stereogram pairs to aid further in interpreting their three-dimensional details. Readers unfamiliar with stereo viewing techniques can simply examine one figure from each pair. To make Figs. 5–8 more readable, we have also labeled the horizon and the maximum view elevation angles in each.

Two caveats about Figs. 5–8 are needed. First, we cannot easily extract two-dimensional information (e.g., chromaticities) from the stereograms, a shortcoming typical of most projections of three-dimensional data plots. Second, to make luminance trends easier to follow, we have linearly rescaled luminances in each figure to different origins and ranges. What we have gained by the lost quantitative detail, however, is a far better qualitative sense of the three-dimensional data that underlie Fig. 3.[21]

For example, note that the chromaticity hooks and bends roughly coincide with local maxima or minima of luminance. This pairing is typical of many color

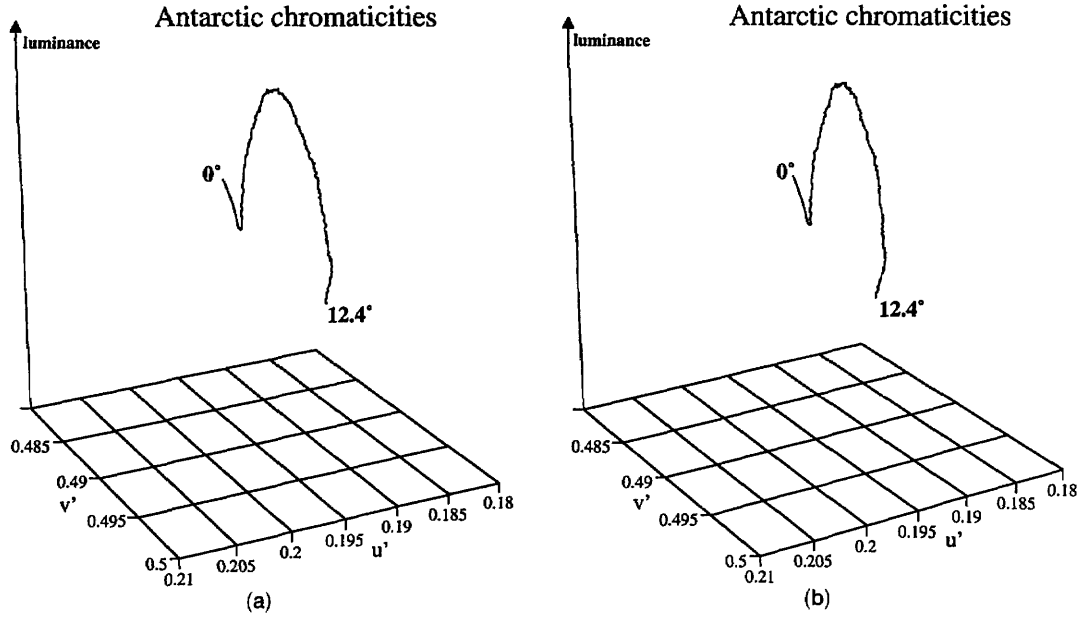

Fig. 6. Stereogram pair of the Antarctic sky's meridional luminance and chromaticity scan (see Ref. 15, Plate 39 for the original photograph).

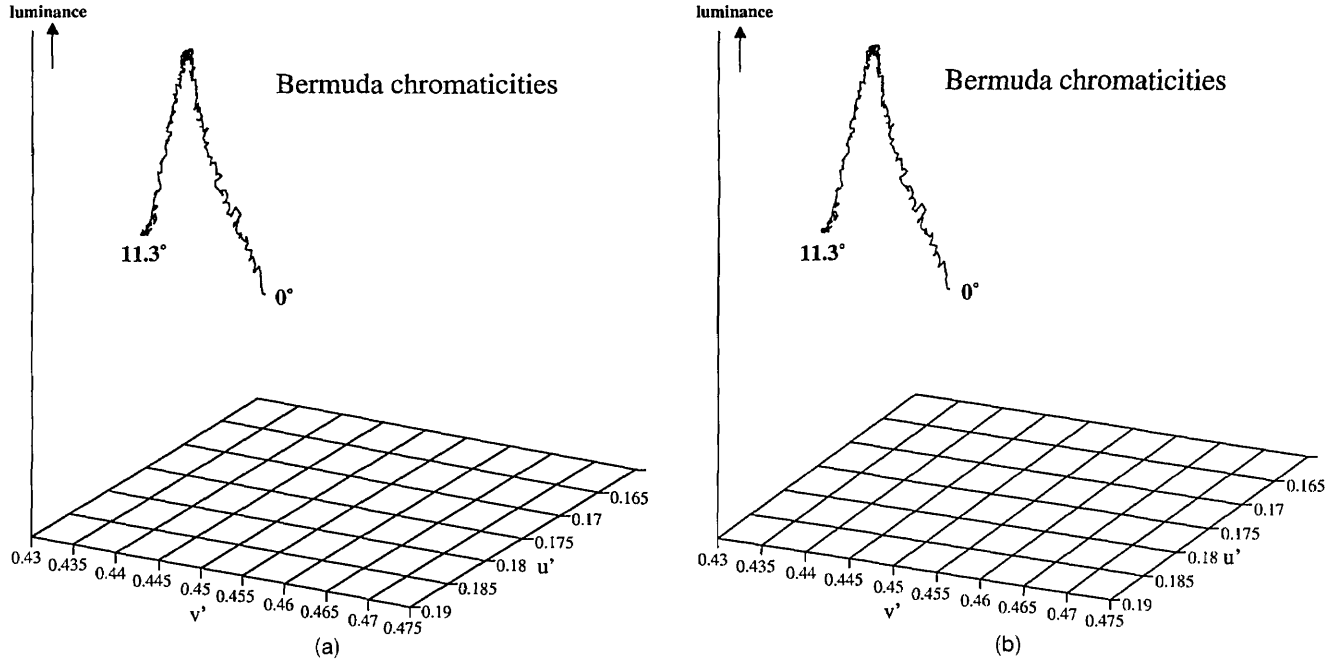

Fig. 7. Stereogram pair of the Bermuda sky's meridional luminance and chromaticity scan (see Ref. 15, Plate 40 for the original photograph).

gradations in nature where, not surprisingly, both luminance and chromaticity change simultaneously. The commingling of luminance and chromaticity changes is least complicated in Fig. 5, in which luminance increases steadily from 19.8°–1.4° elevation, then decreases rapidly toward the horizon. The chromaticity hook at 0.7° elevation nearly coincides with the local luminance maximum.

For the Antarctic sky (Fig. 6), the local luminance maximum and the apex of the chromaticity bend are separated by the same angle as in the Bald Eagle sky: the luminance maximum is at 2.9° and chromaticity changes direction at 2.2° elevation. Below 0.4°, highly reflective snow cover probably causes the luminance increase evident in Fig. 6 (see Fig. 4 also). The pairing of luminance maxima and chromaticity bends persists in the Bermuda (Fig. 7) and the Chesapeake skies (Fig. 8), if somewhat less obviously. In Fig. 7, the luminance maximum is at 5.3° elevation, ~0.7° higher than the chromaticity bend. For the very

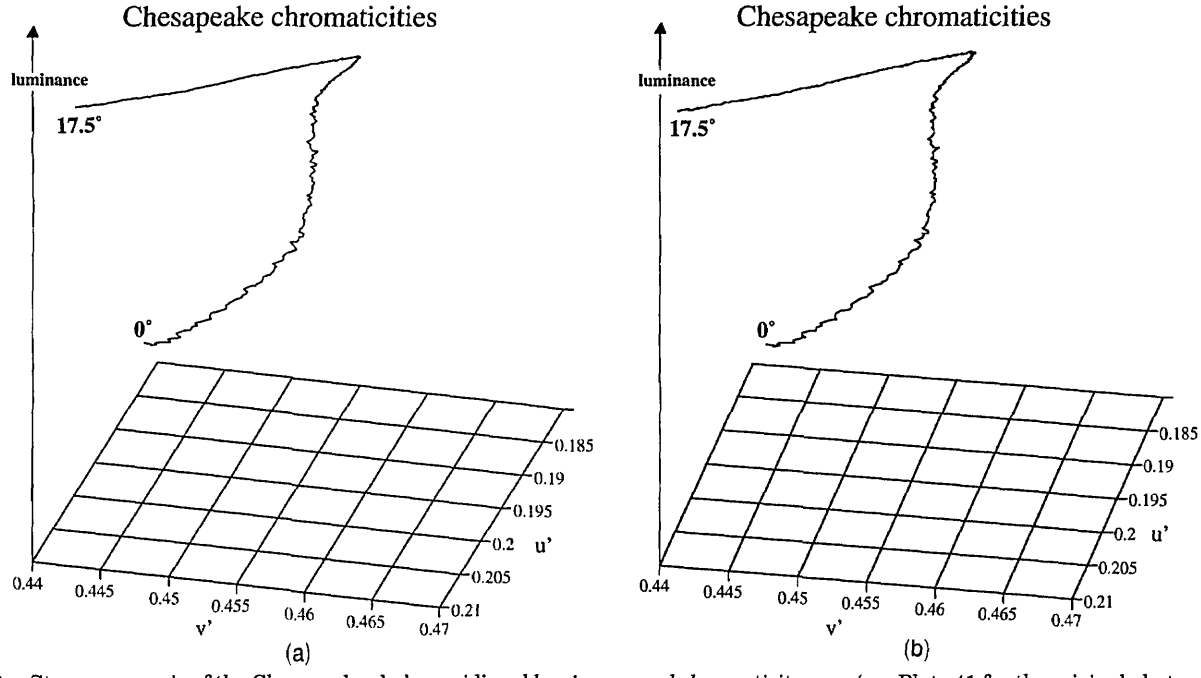

Fig. 8. Stereogram pair of the Chesapeake sky's meridional luminance and chromaticity scan (see Plate 41 for the original photograph).

broad Chesapeake maximum, we simply note that the peak luminance at 8.3° occurs within the 9°–2.5° chromaticity bend.

Graphically, the explanation of the chromaticity hooks and bends is now obvious. Whenever we project a three-dimensional curve of luminances and chromaticities (e.g., Fig. 6) onto a plane, the bends seen in Fig. 3 result. Even if only a single luminance maximum occurs near the horizon (see Figs. 5, 7, and 8), sudden direction changes may occur in the chromaticity plane. Note that the apex of each chromaticity bend corresponds to a purity minimum above the horizon, depending on our choice of achromatic point in Fig. 3. This suggests that the elevated purity minimum seen in Fig. 1 is the rule, rather than the exception.

Physically, a satisfactory quantitative explanation of the near-concurrent color and luminance changes requires further study. Qualitatively, however, we make the following suggestion: changes in the scattering source function and in direct-beam attenuation often lead to a near-horizon radiance maximum.[15] Assuming that these changes are not wavelength independent, we will see nearly coincident (and subtle) changes in skylight's color and luminance just above the horizon.

Some Observed Colors of Clear Twilight Skies

We expect twilight skies to be more impressive visually than daytime skies. Anecdotal evidence for this assumption is amateur photographers' penchant for entering sunset pictures, rather than blue sky pictures, in photography contests. Table 1 demonstrates, that this bias is often justified: $\hat{g}$ ranges from 0.013–0.083 for our five daytime skies, yet it can be many times larger during twilight ($\hat{g}$ = 0.131–0.172 for Plates 42 and 43).

Strictly speaking, however, the clearest blue skies may have much larger color gamuts than the most pedestrian twilights. For example, Plate 41 was taken only minutes before sunset. While the scene does not qualify astronomically as twilight, it certainly does visually. Plate 38 in Ref. 15 is unambiguously a daytime clear-sky scene, yet its $\hat{g}$ (0.083) is nearly three times as large as Plate 41's $\hat{g}$ (0.0281). What Plate 38 lacks, of course, is a wide range of readily identifiable hues (or, in our usage, dominant wavelengths). As uncommon as Plate 38's range of blues is, the fact that we see clear twilights less often than blue skies means that almost any twilight will seem more noteworthy than the purest blue sky.

When we plot the chromaticities of Plates 42 and 43, we find some further surprises (see Fig. 9). Plate 43 was taken approximately six months after the 12–13 June 1991 eruptions of Mt. Pinatubo in the Philippines. As Meinel and Meinel note, volcanic material injected into the stratosphere is a likely cause of spectacular posteruption twilights.[22] Whatever its source, Plate 43's evening twilight is unusually vivid, as its $\hat{g}$ value of 0.131 attests. In comparison, the most vivid rainbow analyzed in Ref. 14 had $\hat{g}$ = 0.0507, some 2.5 times smaller.

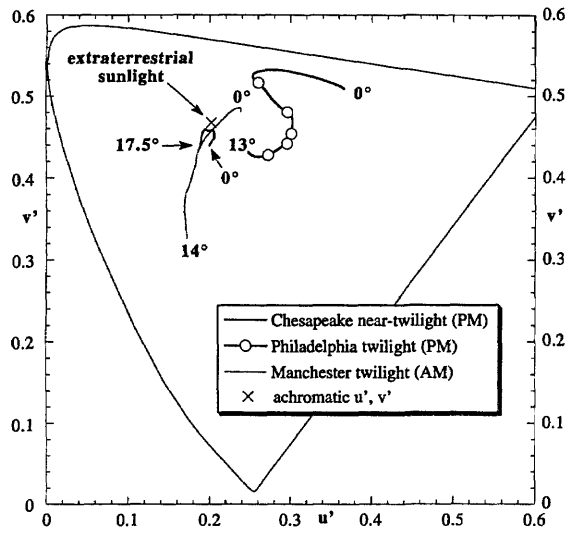

Fig. 9. Chromaticity curves of twilight clear skies from Plate 42 (Manchester, N.H.) and Plate 43 (Philadelphia, Pa.) are compared with the near-twilight sky of Plate 41 (Chesapeake). AM and PM denote morning and evening twilights, respectively. See Fig. 10 for a detailed view of these curves.

However, Plate 42's more pedestrian twilight has an even *larger* $\hat{g}$ of 0.172. How can this be? As Fig. 9 makes clear, $\hat{g}$ does not depend on high purities, merely on having a wide range of chromaticities, many of which may be of comparatively low purity. That $\hat{g}$ sometimes fails to agree with our qualitative impression of color gamut is less an indictment of $\hat{g}$ than a recognition that chromaticity is not a perfect metric of color sensation. Figure 9 also includes the near-twilight chromaticities of Plate 41, which now quite literally pales in comparison to Plates 42 and 43. Because twilight's chromaticity and luminance change fairly rapidly across azimuth,[23] we have reduced the angular width of our azimuthal averages for these three plates (see Table 1).

Figure 10 demonstrates just how much twilight chromaticities can differ from one another. In fact, if Fig. 10 were unlabeled, its variety would leave us hard pressed to identify the sky feature being analyzed. Thus twilight skies are even more loosely related than daytime skies are to the blackbody locus. This colorimetric freedom is not surprising, for during twilight we must consider highly variable spectral scattering and absorption of sunlight that has been transmitted and scattered over very long optical paths. Qualitatively, Fig. 10 agrees well with Minnaert's descriptions of twilight colors.[24]

Figures 11 and 12 confirm that the yellow twilight arch[25] is the brightest part of Plate 43. The elevation of the arch's luminance maximum is 1.7°, and its half-maximum elevations are 0.2° and 5.1° (i.e., the elevations at which luminance has fallen to half the maximum value). Compared to the daytime near-horizon radiance maximum (see Ref. 15, Figs. 6–10), the twilight arch is a much more sharply defined feature. In none of our daytime scenes (Plate 41 and Ref. 15, Plates 37–40) do radiances fall to half-

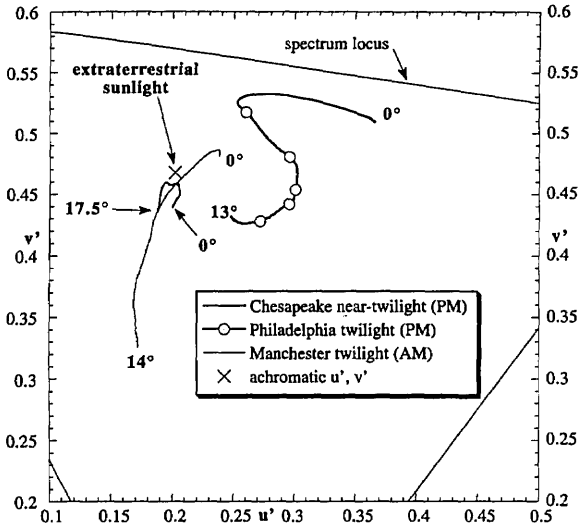

Fig. 10. Detailed view of Fig. 9's twilight chromaticity curves, labeled with view elevation angles corresponding to the horizon and the upper edges of Plates 41–43.

maximum values for a 6° elevation increase. By contrast, even Plate 42's pastel antitwilight sky has a greater luminance dynamic range: its half-maximum elevation is 6.6°, only 5.5° higher than the brightest part of the sky. Not surprisingly, differences in scattering geometry between daytime and twilight help explain these differences in luminance dynamic range (for example, see Ref. 24, pp. 302–303).

Pitfalls in Measuring and Modeling Twilight Colors

After Mt. Pinatubo's 1991 eruptions, Deshler *et al.* made *in situ* measurements of stratospheric aerosols, finding that aerosol surface area "quickly increase[d] by a factor of 10 to 20 throughout the stratosphere below 25 km," compared with pre-eruption background levels.[26] They observed maximum aerosol loading ~150 days after the eruptions (~9 November 1991) and note that after this date the Pinatubo aerosols at their site became more uniformly distributed within the lower stratosphere. Plate 43 was photographed 198 days after the Pinatubo eruptions (27 December 1991). If we assume that Deshler *et al.*'s aerosol history (see their Fig. 4) is representative of that at Plate 43's midlatitude location, then the Pinatubo aerosols likely contributed to Plate 43's vivid colors.

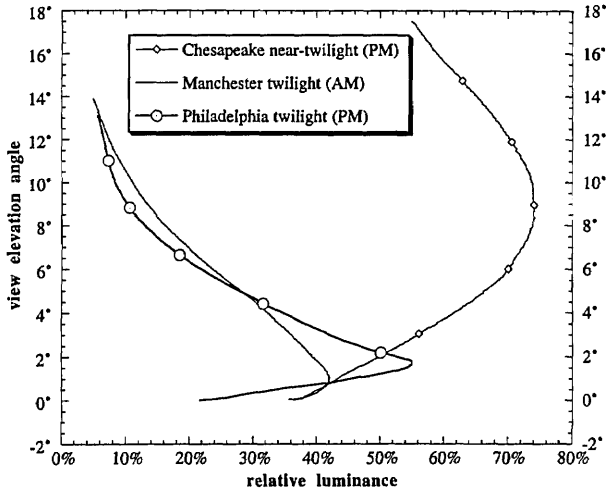

Fig. 11. Relative luminance versus view elevation angle for Plates 41–43. Compare the Philadelphia twilight's relative luminances with their stereo representation in Fig. 12.

At twilight's highest purities, colorimetric saturation of our slide film could slightly compress Fig. 10's meridional chromaticity gamuts. However, the true twilight gamuts are unlikely to expand to the heroic dimensions drawn by Hall[12] and Adams *et al.*[13] In Fig. 13, we examine this claim by translating Hall's Fig. 1 meridional twilight scan to the CIE 1976 UCS diagram and superimposing it on our Fig. 10 chromaticities. Hall's data and ours are not completely comparable because our maximum view elevations are 13°–14°, whereas Hall's observations extend to the zenith. In addition, Hall analyzed a different twilight than ours, so the curves may differ simply because of changed stratospheric aerosol loading.[27] With these caveats in mind, we begin a cautious comparison.

First, note that Hall's twilight chromaticities are based on *in situ* color matching, and thus may be subject to the problems of matching colors under highly chromatic illumination (these problems include simultaneous color contrast and purity overestimates). For example, in Fig. 13, Hall's estimate of zenith purity exceeds 80%. Even allowing for spectral absorption by ozone, such a purity seems unrealistically high. On the other hand, Hall's chromaticity for the solar horizon is more plausible, and certainly is comparable with our analysis of Plate 43. However, Hall's chromaticities yield an estimated horizon-to-horizon twilight $\hat{g}$ of ~0.35, a number not likely found in nature.

Second, our twilight meridional scans are not congruent with Hall's. Differences in atmospheric scattering and absorption will account for some of the shape differences. However, for small solar depression angles, the S-shaped chromaticity curve of the Philadelphia data seems more plausible than does Hall's smooth progression from pure reds to pure blues. By contrast, the sequence of twilight color names in Minnaert's Fig. 169 (at 4° solar depression) suggests the kind of dominant wavelength sequence seen in our Philadelphia chromaticities.[24] If Hall's chromaticities are based on his Plate 116, then our Plate 41 and its M-shaped chromaticity curve (Fig. 3) better describe his observations.

Our point here is not a criticism of Hall's particular results, but of relying exclusively on naked-eye observations when quantifying sky color. Understandably, in 1979 Hall was struggling with the measurement problem described above: low-light phenomena such as twilight colors could not be measured instrumentally. Hall notes that Adams *et al.*'s[13] single-scattering models of twilight colors (for example, see

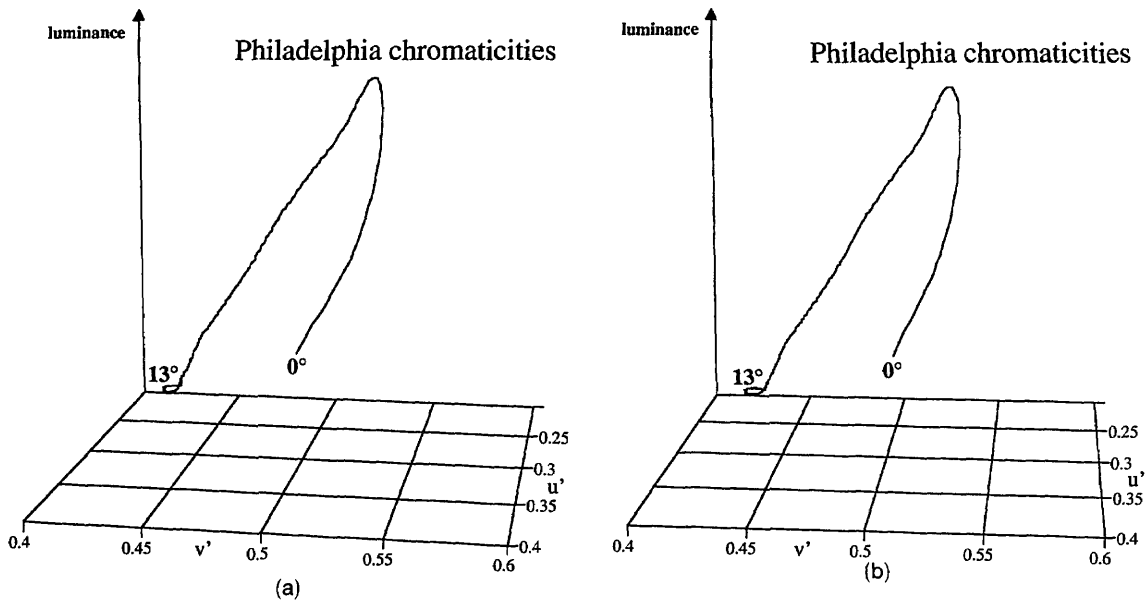

Fig. 12. Stereogram pair of the Philadelphia twilight sky's meridional luminance and chromaticity scan (see Plate 43 for the original photograph).

their Fig. 21) are similar to his observations along the solar, but not the antisolar, meridian. However, this agreement seems to be a case of unrealistic models bolstering inaccurate observations. Figure 13 suggests that, in general, neither naked-eye observations nor single-scattering models can adequately describe twilight chromaticities.

Conclusions

Developing a physical model of clear-sky colors is the obvious next step in our work. Almost certainly, we need to begin with a multiple-scattering model such as the second-order scattering model described in Ref. 15. For the most spectacular sunsets, ozone and other absorbing constituents also need to be considered in some detail. For now, however, what new things have we learned about clear-sky colors?

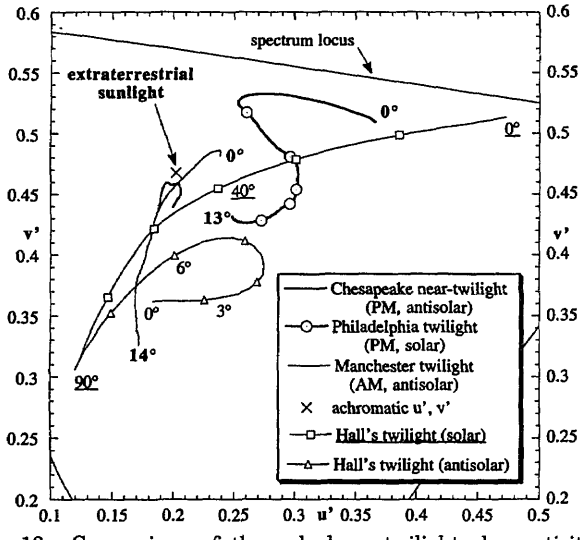

Fig. 13. Comparison of the naked-eye twilight chromaticities reported by Hall (Ref. 12, Fig. 1) and those plotted in Fig. 10. View elevation angles are labeled for most curves. The labels solar and antisolar indicate the relative azimuth of each meridional scan.

First, we now know that skylight colors have a wide range of chromaticities and meridional chromaticity curves. Unlike daylight scattergrams, skylight meridional chromaticity curves will only occasionally resemble the blackbody locus. Any confusion of skylight and daylight colors can be clarified by examining Fig. 3. Second, small-scale chromaticity bends are characteristic of daytime clear-sky meridional scans, and these bends approximately coincide with local luminance maxima found above the horizon. A corollary discovery is that clear daytime skies have purity minima a small distance above the horizon (i.e., near their luminance maxima), rather than at the horizon. In short, we cannot divorce luminance changes from chromaticity changes if we want to understand clear-sky colors satisfactorily. Third, colorimetric gamut $\hat{g}$ is usually much larger for twilight than for daytime clear skies, as we would expect. However, very clear blue skies will span a broader color range than some twilights, even if the blue skies do not *seem* more impressive. Fourth, our results reaffirm my earlier claim that few phenomena in atmospheric optics have both a large color gamut and high colorimetric purity.[14] The notable exception to this rule here is the Philadelphia twilight (Plate 43), and it seems to be the result of very unusual atmospheric conditions.

Finally, what can we say of Bohren and Fraser's opening gibe? We trust that our results, like theirs, make clear that no date is too late for a fruitful study of clear-sky colors. As familiar as we may be with noon's azure sky or the spectacular hues of twilight, neither one is yet devoid of surprises.

This work was supported by National Science Foundation grant number ATM-8917596. Alistair Fraser and Craig Bohren of Penn State have offered useful (and compelling) intellectual nudges. I am indebted to Michael Churma of Penn State, who made the radiometer measurements seen in Fig. 1 and who provided me with Plate 37 in Ref. 15. Stephen Mango and colleagues at the U.S. Naval Research Laboratory's Washington, D.C. Center for Advanced Space Sensing have provided generous support of this project, as has the U.S. Naval Academy Research Council.

References and Notes

1. C. F. Bohren and A. B. Fraser, "Colors of the sky," Phys. Teach. **23,** 267–272 (1985).
2. E. R. Dixon, "Spectral distribution of Australian daylight," J. Opt. Soc. Am. **68,** 437–450 (1978).
3. V. D. P. Sastri and S. R. Das, "Typical spectral distributions and color for tropical daylight," J. Opt. Soc. Am. **58,** 391–398 (1968).
4. V. D. P. Sastri and S. R. Das, "Spectral distribution and color of north sky at Delhi," J. Opt. Soc. Am. **56,** 829–830 (1966).
5. G. T. Winch, M. C. Boshoff, C. J. Kok, and A. G. du Toit, "Spectroradiometric and colorimetric characteristics of daylight in the southern hemisphere: Pretoria, South Africa," J. Opt. Soc. Am. **56,** 456–464 (1966).
6. D. B. Judd, D. L. MacAdam, and G. Wyszecki, "Spectral distribution of typical daylight as a function of correlated color temperature," J. Opt. Soc. Am. **54,** 1031–1040 (1964).
7. H. R. Condit and F. Grum, "Spectral energy distribution of daylight," J. Opt. Soc. Am. **54,** 937–944 (1964).
8. Y. Nayatani and G. Wyszecki, "Color of daylight from north sky," J. Opt. Soc. Am. **53,** 626–629 (1963).
9. Daylight terminology is confusing at best, although some authors have tried to codify it. See, for example, G. Wyszecki and W. S. Stiles, *Color Science: Concepts and Methods, Quantitative Data and Formulae* (Wiley, New York, 1982), p. 11.
10. R. L. Lee, Jr., "Colorimetric calibration of a video digitizing system: algorithm and applications," Col. Res. Appl. **13,** 180–186 (1988).
11. We used a Photo Research PR-704 spectroradiometer with a nominal 0.5° FOV.
12. F. F. Hall, Jr., "Twilight sky colors: observations and the status of modeling," J. Opt. Soc. Am. **69,** 1179–1180, 1197 (1979).
13. C. N. Adams, G. N. Plass, and G. W. Kattawar, "The influence of ozone and aerosols on the brightness and color of the twilight sky," J. Atmos. Sci. **31,** 1662–1674 (1974).
14. R. L. Lee, Jr., "What are 'all the colors of the rainbow'?" Appl. Opt. **30,** 3401–3407, 3545 (1991). The 1991 printing of Eq. (1) inadvertently omitted the overbars; the reported $\hat{g}$ values are correct, however.
15. R. L. Lee, Jr., "Horizon brightness revisited: measurements and a model of clear-sky radiances," Appl. Opt. **33,** 4620–4628 (1994).
16. These achromatic stimuli are derived from the extraterrestrial solar irradiances reported by M. P. Thekaekara, "Solar energy outside the earth's atmosphere," Sol. Energy **14,** 109–127 (1973).
17. "Relative azimuth" here means azimuth measured with respect to the Sun's azimuth; a relative azimuth of 0° points toward the Sun's azimuth. For the hemispheric daylight chromaticities shown in Figs. 1 and 3, 0° relative azimuth was defined by tilting the surface normal of the radiometer's cosine detector at an angle of 75° from the zenith and by pointing this surface normal toward the Sun's azimuth.
18. G. J. Burton and I. R. Moorhead, "Color and spatial structure in natural scenes," Appl. Opt. **26,** 157–170 (1987).
19. C. J. Bartleson, "Memory colors of familiar objects," J. Opt. Soc. Am. **50,** 73–77 (1960).
20. Readers unfamiliar with three-dimensional color spaces and color solids may consult Secs. 3.3.9–3.7 of Ref. 9.
21. We have not shown a stereogram for the University Park, Pa., chromaticities (Ref. 15, Plate 37) because their noisiness and broad luminance maximum make stereo interpretation difficult.
22. A. Meinel and M. Meinel, *Sunsets, Twilights, and Evening Skies,* (Cambridge U. Press, Cambridge, 1983), pp. 51–61. Reference 23 offers a more comprehensive survey of twilight optics.
23. G. V. Rozenberg, *Twilight: A Study in Atmospheric Optics* (Plenum, New York, 1966).
24. M. G. J. Minnaert, *Light and Color in the Outdoors,* translated and revised by L. Seymour (Springer-Verlag, New York, 1993), pp. 295–297.
25. Strictly speaking, the twilight arch is defined only for solar depression angles of ~7°–16°. See, for example, H. Neuberger, *Introduction to Physical Meteorology* (Penn State Press, University Park, Pa., 1957), p. 185. However, the yellow band in Plate 43 (solar depression ~2°) is a local luminance maximum, and it remained so for solar depression angles > 7°.
26. T. Deshler, B. J. Johnson, and W. R. Rozier, "Balloonborne measurements of Pinatubo aerosol during 1991 and 1992 at 41° N: vertical profiles, size distribution, and volatility," Geophys. Res. Lett. **20,** 1435–1438 (1993).
27. Although the twilight seen in Hall's Plate 116 (dated 17 August 1978; see Ref. 12) may be the basis for his Fig. 1, Hall does not state this unambiguously, thus making the issue of stratospheric aerosol loading moot for his data. In any case, the pastel colors of Hall's Plate 116 are quite different from those of vivid posteruption twilights (e.g., our Plate 43).